

***In Silico* Study of Bioactive Compounds from Red Fruit (*Pandanus conoideus* Lamk.) as Inhibitors of Human Alcohol Dehydrogenase**Dedy N. Hidayat^{1,2}, Gita V. Soraya^{1,3}, Rosdiana Natzir^{1,3}, Syahrijuita Kadir^{1,3}, Andrian Sucahyo⁴, Herlina Yulidia², Marhaen Hardjo^{1,3 *}¹Master Program of Biomedical Sciences, Graduate School, Hasanuddin University, Makassar, South Sulawesi, Indonesia²Faculty of Medicine, University of Papua, Sorong, Southwest Papua, Indonesia³Department of Biochemistry, Faculty of Medicine, Hasanuddin University, Makassar, South Sulawesi, Indonesia⁴Faculty of Mathematic and Natural Science, Essential Oil Institute, Brawijaya University, Malang, East Java, Indonesia**ARTICLE INFO****ABSTRACT****Article history:**

Received 03 November 2025

Revised 01 December 2025

Accepted 04 December 2025

Published online 01 January 2026

Copyright: © 2025 Hidayat *et al.* This is an open-access article distributed under the terms of the [Creative Commons Attribution License](#), which permits unrestricted use, distribution, and reproduction in any medium, provided the original author and source are credited.

Alcohol addiction and intoxication are serious global health issues, primarily influenced by the metabolic conversion of ethanol into acetaldehyde. This toxic substance causes various harmful effects on the liver, including alcoholic fatty liver (steatosis), steatohepatitis, fibrosis, and hepatocellular carcinoma. Meanwhile, alcohol dehydrogenase (ADH) enzyme facilitates the initial metabolic process. Inhibiting ADH is a potential therapeutic method to slow alcohol metabolism and reduce the side effects of acetaldehyde. Fomepizole is an efficient ADH inhibitor, and the use is limited due to several side effects and high costs, signifying the need to explore safer alternatives. Therefore, this study aimed to investigate the efficacy of bioactive compounds from *Pandanus conoideus* Lamk. (red fruit), an endemic plant from Papua, Indonesia, as potential ADH inhibitors using *in silico* methods. Molecular docking simulations and molecular dynamics were used to evaluate the compounds and identify the most promising candidates. Among the compounds evaluated through molecular docking, several flavonoids, such as 3,4',5-trihydroxy-7,3'-dimethoxy flavone (TDF) and taxifolin (TX), had the highest binding affinity scores towards ADH at -7.3 kcal/mol. The next compound producing the highest binding affinity score was quercetin (QE), with a value of -7.1 kcal/mol. Molecular dynamics simulations lasting more than 50 ns signified that QE was the most stable ligand, with root-mean-square deviation (RMSD) value that remained below 5 Å. The results generally showed that only QE from *Pandanus conoideus* had potential as ADH inhibitor.

Keywords: *Pandanus conoideus*, *In silico*, Human Alcohol Dehydrogenase Inhibitors**Introduction**

Alcohol abuse is a serious global health issue, leading to various medical conditions, such as liver disease, cardiovascular disorders, and certain cancers.^{1,2} The basic mechanism of alcohol metabolism in the body, which primarily occurs in the liver, includes three main enzymatic pathways consisting of alcohol dehydrogenase (ADH), microsomal ethanol oxidation system (MEOS) mediated by cytochrome P450 enzymes, and *catalase*.³ Furthermore, ethanol oxidation is the primary phase and rate-limiting step, majorly facilitated by class I alcohol dehydrogenase (ADH1), which produces acetaldehyde, a toxic compound responsible for the adverse health effects associated with excessive alcohol consumption.⁴ The conversion of ethanol to acetaldehyde is often facilitated by ADH, a zinc-dependent metalloenzyme that exists as a dimer in humans.^{5,6} Zinc atom in ADH is crucial for the activity of the enzyme through binding to alcohol hydroxyl group, thereby positioning for oxidation. This is classified as an oxidation-reduction (redox) reaction, which requires the presence of nicotinamide adenine dinucleotide (NAD⁺).

*Corresponding author. E mail: marhaenhardjo@unhas.ac.id
Tel: +62 853 4485 4679

Citation: Hidayat DN, Soraya GV, Natzir R, Kadir S, Sucahyo A, Yulidia H, Hardjo M. *In Silico* Study of Bioactive Compounds from Red Fruit (*Pandanus conoideus* Lamk.) as Inhibitors of Human Alcohol Dehydrogenase. Trop J Nat Prod Res. 2025; 9(12): 6056 – 6064 <https://doi.org/10.26538/tjnpr/v9i12.20>

Official Journal of Natural Product Research Group, Faculty of Pharmacy, University of Benin, Benin City, Nigeria

During the process, ADH interacts with ethanol and NAD⁺, then the enzyme catalyzes the extraction of hydride ions (hydrogen atoms with two electrons) from ethanol molecule and transfers the extract to NAD⁺.^{7,8} This process simultaneously oxidizes ethanol into acetaldehyde while reducing NAD⁺ to the electron-transferring form, NADH. Inhibiting ADH slows alcohol metabolism, reduces acetaldehyde formation, and may alleviate the intensity of the harmful effects.⁹ ADH oxidizes accidentally ingested methanol to become formaldehyde, which is converted into highly toxic formic acid. Similarly, ADH converts ethylene glycol into glycoaldehyde, which is oxidized into glycolic acid, the primary factor in severe metabolic acidosis observed in poisoning. In both cases, the toxic metabolites, not the original alcohol, are responsible for the severe and often fatal consequences impacted on the body.

Fomepizole is a competitive inhibitor of ADH with proven clinical efficacy, which acts by reversibly binding to the active site of the enzyme and blocking the substrate metabolism.¹⁰ This drug inhibits the transformation of parent alcohols into harmful metabolites, facilitating the safe elimination. However, fomepizole presents disadvantages in the form of adverse effects such as headaches, nausea, dizziness, and transient elevations in liver enzymes, significant expense, and the need for intravenous (IV) delivery during administration.¹¹ The disadvantages show the critical demand for novel, more efficacious, safer, and cost-effective ADH inhibitors.¹² Therefore, new ADH inhibitors need to be derived from natural products due to the potential for fewer side effects compared to the known ADH inhibitors.¹³

Pandanus conoideus Lamk., commonly known as "red fruit," is a native plant of Papua (Indonesia) with a broad spectrum of pharmacological activities, including antioxidant, antibacterial, antihyperglycemic, anti-inflammatory, and anticancer properties.^{14,15,16} *Pandanus conoideus* is

rich in carotenoids and flavonoids.^{17,18} The primary carotenoid compounds found in *Pandanus conoideus* are β -carotene, followed by capsanthin 5,6 epoxide, capsanthin 3,6 epoxide, 5,6-diepicapsokarpoanthin, β -kryptoxanthin 5,6-epoxide, kapsorubin, kapsantin, kriptokapsin, β -Kriptoksantin, α -cryptoxanthin, and capsanthin 5,8 epoxide.^{19,20} This plant is also rich in flavonoids, such as 4',6,6',8-tetrahydroxy-3-methoxy-flavone (TMF), 3,4',5-trihydroxy-7,3'-dimethoxy flavone (TDF), taxifolin (TX) 3-*O*- α -arabinopyranoside, isoquercetin, 3-*O*-methylquercetin, quercetin (QE), TX, quercetin-3'-glucoside, rutin, astragalol, and trifolin, as well as fatty acids.^{19,21,22}

The potential roles of *Pandanus conoideus* as ADH inhibitor have not been investigated despite the recognition of the diverse pharmacological activities, including antioxidant, antibacterial, antihyperglycemic, anti-inflammatory, and anticancer properties. Therefore, this study represents the first attempt to explore the inhibitory activity of bioactive compounds from *Pandanus conoideus* against ADH, filling a critical gap in the search for natural product-based strategies to mitigate alcohol-related toxicity. The novelty of this study lies in the unique focus on a traditional Papuan medicinal plant as a potential source of safer and more affordable ADH inhibitors, different from existing synthetic options such as fomepizole limited by adverse effects, high cost, and intravenous administration requirements. Although the medicinal plant is known to contain abundant bioactive flavonoids and carotenoids, there has been no scientific evidence clarifying the molecular processes by which these compounds engage with the human ADH enzyme. The binding affinity, active site interactions, and dynamic stability of Red Fruit metabolites remain

uncharacterized. The lack of molecular-level data establishes a significant knowledge gap, hindering the validation of this endemic Papuan plant as an effective natural competitive inhibitor for alleviating alcohol-induced toxicity.

Materials and Methods

This study used various software tools for the analysis process, including AutoDockTools-1.5.6 and Autodock Vina 4.2 from the Scripps Research Institute (2012), Swiss ADME (<http://www.swissadme.ch>), and Chimera V.1.18 (Resources for Bioinformatics, Visualization, and Informatics, 2023). Other tools were ChemOffice (Revvity Signals, 2023), Biovia Discovery Studio 2025 (Dassault Systèmes), Open Babel, Gromacs 2025.2 (Herman Berendsens Group), and ADMET-AI (<https://admet.ai.greenstonebio.com>).

Drug-ADMET Compatibility Testing

Bioactive compounds of *Pandanus conoideus* obtained from previous studies for drug-ADMET compatibility testing are shown in Figure 1.^{19,21} All compounds were analyzed by using SMILES identifications in Swiss ADME (<https://www.swissadme.ch>) to determine the pharmacological properties and ADME properties. Additionally, SMILES identifications were analyzed using ADMET-AI (<https://admet.ai.greenstonebio.com>) to obtain the overall ADMET property radial graphs of the active compounds.²³

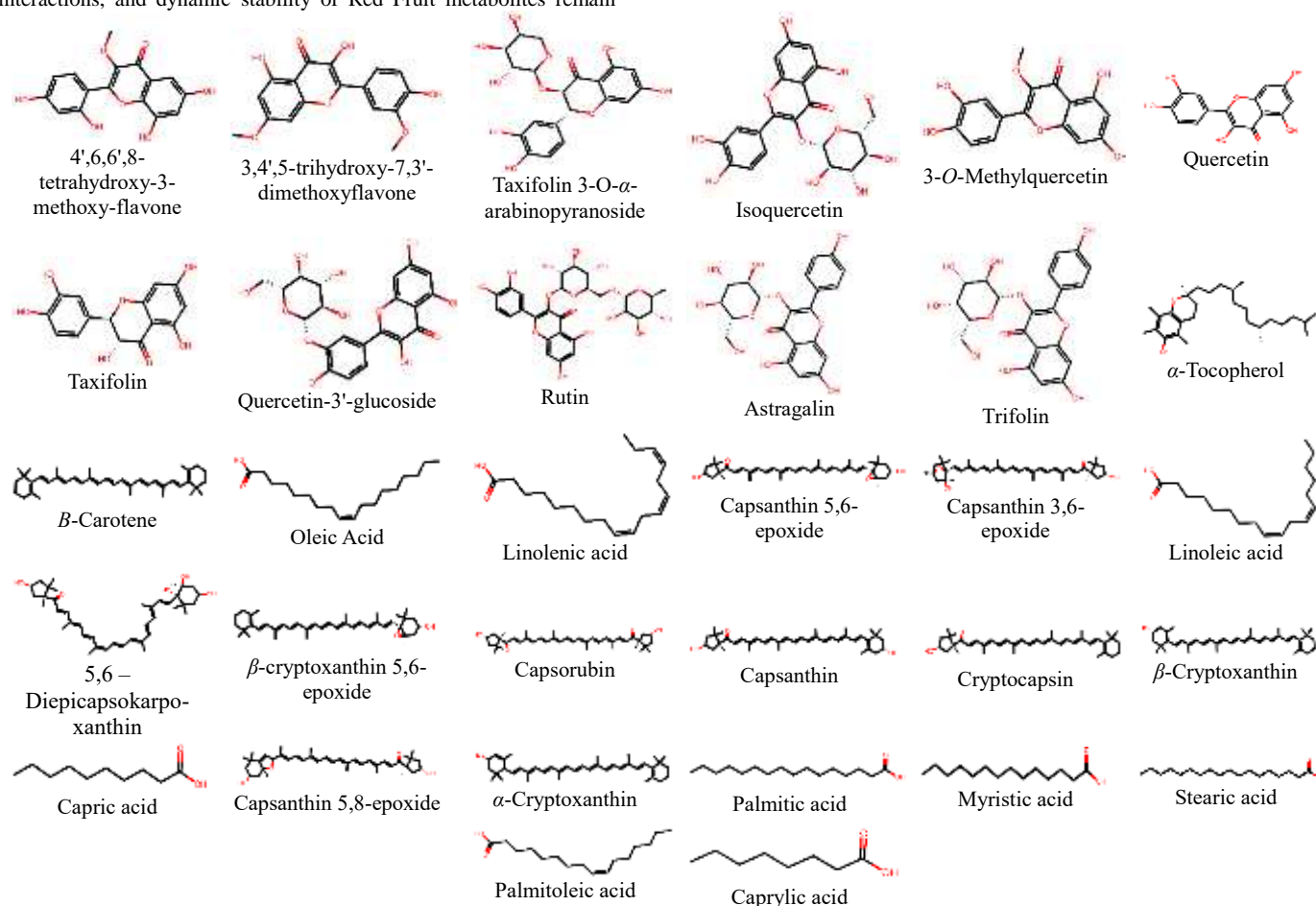


Figure 1: The active chemical compounds from *Pandanus conoideus* Lamk.

Molecular Docking Study

Identifying suitable receptors is the initial step in conducted *in silico* drug screening. ADH protein was downloaded from RCSB PDB database (<https://www.rcsb.org>) with PDB ID 1HDZ. Protein was prepared using AutoDockTools-1.5.6 by removing water molecules and

heteroatoms, including the addition of Kollman charges, and the introduction of polar hydrogen.²⁴ Missing residues were corrected using the DockPrep tool in the Chimera program v1.18. All ligands used in this study were downloaded in SDF file format (3D conformation), structurally optimized using MM2 method in Chem3D 23.1.1, and

converted to PDB format. Subsequently, molecular docking studies were performed using Autodock Vina to provide binding affinity data and PDBQT files for complex visualization in BioVia Discovery Studio 2025. The grid used was centered around NAD molecule, specifically

at -6.628, 11.412, and -32.13 (center-x, center-y, and center-z), as shown in Figure 2. NAD molecule as a native ligand of 1HDZ was separated from the protein and re-docked for method validation with the same procedure used for other compounds.^{25,26}

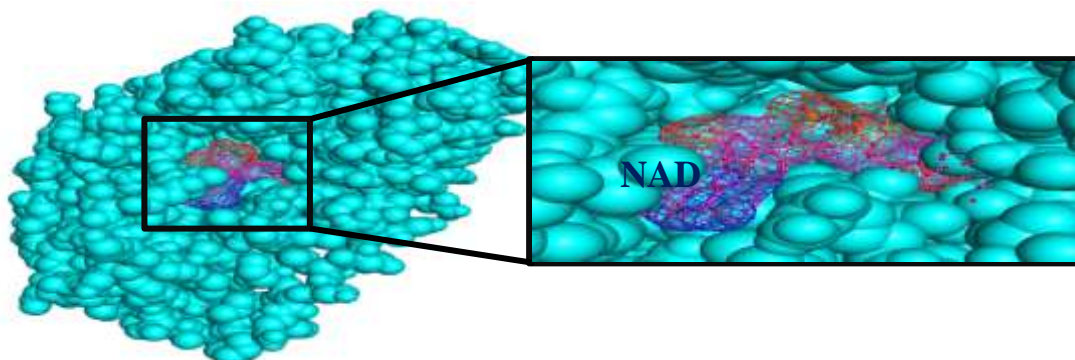


Figure 2: Location of the active site of ADH protein near NAD molecule (lattice structure).

Molecular Dynamics

The ligands generated from the docking procedure were converted to the (.mol2) format using Open Babel and re-optimized by adding all hydrogen atoms. Subsequently, the entire ligands were prepared for topology using the SwissParam server with MMFF-based method. Molecular dynamics (MD) simulations were performed using Gromacs 2025.2, which applied the Charmm27 force field and single-point charge (SPC) water model, followed by neutralization with Cl⁻ or Na⁺ counter ions. Protein energy minimization was carried out with 5,000 iterations of the steepest descent method. NVT and NPT equilibration, each lasting 100 ps, were performed after the energy minimization process. Molecular docking simulations were performed for 50 ns at 300 K, and the simulation trajectories obtained were analyzed using the Xmgrace program to calculate root-mean-square deviation (RMSD), root-mean-square fluctuation (RMSF), hydrogen bonds, and radius of gyration (Rg) of protein-ligand complex.²⁷

Results and Discussion

Druglikeness Screening

The Lipinski rules serve as a crucial screening method in drug development to assess the "drug-like" characteristics of a compound. These rules consist of several criteria to predict the likelihood of a compound possessing the physicochemical properties required for optimal oral absorption and permeability. The guidelines state that a molecule should not exceed one violation of the following criteria to have good oral bioavailability: 1) molecular weight below 500 Dalton, 2) calculated lipophilicity not exceeding 5, 3) maximum of 5 hydrogen bond donors, and 4) maximum of 10 hydrogen bond acceptors. An additional rule commonly used is TPSA (*Topological Polar Surface Area*) $\leq 140 \text{ \AA}^2$, because of the relationship with membrane permeability.²⁸ Table 1 shows that all carotenoids isolated from *Pandanus conoideus* Lamk. do not meet the Lipinski rules due to the high molecular weight (MW). Molecules with high MW have difficulty penetrating the lipid bilayer of intestinal cell membranes, and this reduced permeability leads to fewer drugs entering the bloodstream.²⁹ A few active compounds have characteristics similar to oral drugs, namely TMF, TDF, QE, TX, capric acid, myristic acid, and caprylic acid. All compounds that passed the Lipinski screening rules passed through further *in silico* analysis.

Table 1: Drug similarity screening of active compounds from *Pandanus conoideus* Lamk. using Lipinski's rules

Compound	MW	LogP	HBD	HBA	TPSA	Violation
Flavonoid						
4',6,6',8-tetrahydroxy-3-methoxy-flavone	316.26	2.29	4	7	120.36	0
3,4',5-trihydroxy-7,3'-dimethoxyflavone	330.29	2.59	3	7	109.36	0
Taxifolin 3- <i>O</i> - α -arabinopyranoside	436.37	-0.35	7	11	186.37	2
isocwerketin	464.38	-0.54	8	12	210.51	2
3- <i>O</i> -methylquercetin	316.26	2.29	4	7	120.36	0
Quercetin	302.24	1.99	5	7	131.36	0
Taxifolin	304.25	1.19	5	7	127.45	0
Quercetin-3'-glucoside	464.38	-0.54	8	12	210.51	2
Regular	610.52	-1.69	10	16	269.43	3
Astragalin	448.38	-0.24	7	11	190.28	2
Trifolin	448.38	-0.24	7	11	190.28	2
Vitamin						
Alpha-Tocopherol	430.72	8.84	1	2	29.46	1
Carotenoids						
β -carotene	536.89	12.61	0	0	0	2
Capsanthin 5,6-epoxide	600.88	9.02	2	4	70.06	2
Capsanthin 3,6 epoxide	600.88	9.02	2	4	66.76	2
5,6 – di-epi-carboxanthin	618.9	7.97	4	5	97.99	2
β -cryptoxanthin 5,6-epoxide	568.89	10.79	1	2	32.76	2
Capsorubin	600.88	9.07	2	4	74.6	2
Capsanthin	584.89	9.81	2	3	57.53	2

Cryptocapsin	568.89	10.84	1	2	37.3	2
β -Cryptoxanthin	552.89	11.58	1	1	20.23	2
α -Cryptoxanthin	552.89	11.43	1	1	20.23	2
Capsanthin 5,8 epoxide	600.88	9.02	2	4	66.76	2
Fatty acid						
Oleic acid	282.47	6.11	1	1	37.3	1
Linolenic acid	278.44	5.66	1	1	37.3	1
linoleic acid	280.45	5.88	1	1	37.3	1
capric acid	172.27	3.21	1	1	37.3	0
Palmitic acid	256.43	5.55	1	1	37.3	1
myristic acid	228.38	4.77	1	1	37.3	0
stearic acid	284.48	6.33	1	1	37.3	1
palmitoleic acid	254.41	5.33	1	1	37.3	1
caprylic acid	144.21	2.43	1	1	37.3	0

Table Notes: MW (Molecular Weight) \leq 500 Da; LogP (logarithm of P, partition coefficient) \leq 5; HBD (Hydrogen Bond Donor) \leq 5; HBA (Hydrogen Bond Acceptor) \leq 10; TPSA (Topological Polar Surface Area) \leq 140 Å².

ADMET and Toxicity

Swiss ADME server (Table 2) shows that all ligands, including the reference inhibitor Fomepizole, present exceptional gastrointestinal (GI) absorption. Great potential of effective absorption into the circulation following oral administration is signified by high GI absorption. However, the profiles differ significantly in other important characteristics. Fomepizole, along with fatty acids Capric acid (CRA),

Myristic acid (MA), and Caprylic acid (CYA), is estimated to penetrate Blood-Brain Barrier (BBB), suggesting potential effects on the central nervous system. Meanwhile, flavonoids such as TMF, TDF, QE, and TX are unable to penetrate the BBB, reducing the potential of central nervous system side effects. There are no active compounds expected to be substrates for P-glycoprotein, signifying favorable results as this implies absence of active excretion from cells.

Table 2: ADMET profile of active compounds from *Pandanus conoideus* Lamk

Standard Parameters	Compound							
	Fomepizole	TMF	TDF	QE	TX	CRA	MA	CYA
GI Absorption	High	High	High	High	High	Height	Height	High
BBB	Yes	No	No	No	No	Yes	Yes	Yes
P-gp substrate	No	No	No	No	No	No	No	No
CYP1A2 inhibitor	No	Yes	Yes	Yes	No	No	Yes	No
CYP2C19 inhibitor	No	No	No	No	No	No	No	No
CYP2C9 inhibitor	No	No	Yes	No	No	No	No	No
CYP2D6 inhibitor	No	Yes	Yes	Yes	No	No	No	No
CYP3A4 inhibitor	No	Yes	Yes	Yes	No	No	No	No

Notes: TMF (4',6,6',8-tetrahydroxy-3-methoxy-flavone); TDF (3,4',5-trihydroxy-7,3'-dimethoxy flavone); QE (Quercetin); TX (Taxifolin); CRA (Capric acid); MA (Myristic acid); CYA (Caprylic acid)

All the described ligands show different inhibitory profiles against several cytochrome P450 (CYP450) enzymes, which are important for drug metabolism. TMF, TDF, and QE can inhibit CYP1A2 and CYP2D6, with TDF potentially affecting CYP2C9. The inhibition may lead to significant drug interactions when the stated drugs are administered concurrently with other drugs metabolized by these enzymes.³⁰ TX has a favorable profile, without inhibiting any CYP450 enzymes, suggesting minimal risk of metabolic drug interactions. Similarly, fatty acids (CRA, MA, CYA) and Fomepizole have negligible to no inhibition of these specific CYP450 enzymes, making the metabolic profiles relatively safer compared to flavonoid compounds such as TMF, TDF, and QE.

The radial plot shows that TDF, QE, and TX have favorable ADMET profiles according to ADMET-AI prediction model (Figure 3). This graph shows the safety and bioavailability predictions of the compounds based on critical criteria.³¹ All three compounds are categorized in the safe range for BBB permeability and hERG inhibition, which are important indicators for central nervous system and cardiovascular safety, respectively.^{32,33} These data present a low probability of causing neurotoxicity or cardiotoxicity. The three compounds show favorable evaluations for non-toxicity and solubility, suggesting minimal risk of general toxicity and a high probability of solubility in biological fluids.

Molecular Docking

The method validation was carried out before proceeding to the investigation of bioactive compounds from *Pandanus conoideus*. The method used in this study was valid because the re-docking process produced RMSD value (1.543 Å) below 2.0 Å, as presented in Figure 4.²⁶ The active chemical compounds analyzed have varying inhibitory activity against ADH enzyme. The most potent inhibitors are TDF and TX, both showing the highest binding affinity scores of -7.3 kcal/mol (Table 3). TDF forms several hydrophobic interactions with amino acid residues such as His51, Ile224, and Gly365, hydrogen bonds with Asp50 and Leu362, and electrostatic interactions with the coenzyme NAD (Figure 5). Both hydrogen bonds and hydrophobic interactions stabilize TDF in ADH enzyme binding site.³⁴ Meanwhile, TX forms hydrogen bonds with Leu362 and NAD molecule. QE and TMF have significant binding affinities (-7.1 and -7.0 kcal/mol, respectively), leading to the consideration as promising ADH inhibitor candidates.

Fatty acids such as Capric Acid (CRA), Myristic Acid (MA), and Caprylic Acid (CYA), along with the positive control (Fomepizole), have lower binding affinities, ranging from -4.2 to -4.5 kcal/mol. These values signify less effective inhibitors compared to flavonoid compounds. Fomepizole, a recognized ADH inhibitor, primarily interacts through hydrophobic interactions with Leu362 and hydrogen bonds with NAD molecules. Fatty acids have greater variability in hydrophobic interactions with different amino acid residues. However, the lower bond scores show that the interactions are less energetically

favorable for sustained bonds compared to the types associated with flavonoids.³⁵

All compounds, except caprylic acid, inhibit the same active site near NAD as fomepizole (Figure 6). This suggests that the five compounds may have a similar mechanism of methanol inhibition to fomepizole in

preventing methanol and ethylene glycol poisoning by interacting with NAD molecules.¹¹ Three molecules with the best binding affinities were further studied using the molecular dynamics method, including TDF, QE, and TX.

Table 3: Bond affinity scores and ligand interactions with ADH

Compound	Binding Affinity (kcal/mol)	Amino Acid Interactions		
		Hydrophobic	Hydrogen Bond	Electrostatic
*Fomepizole	-4.2	Leu362	NAD	-
4',6,6',8-tetrahydroxy-3-methoxy-flavone (TMF)	-7.0	His51, His363, NAD	Ile269, Leu362	-
3,4',5-trihydroxy-7,3'-dimethoxyflavone (TDF)	-7.3	His51, Ile224, Gly365	Asp50, Leu362	NAD
Quercetin (QE)	-7.1	-	Ser54, Lys228, NAD	-
Taxifolin (TX)	-7.3	-	Leu362, NAD	-
Capric acid (CRA)	-4.4	His51, Ile269, Leu362, His363	Asn225, Lys228, NAD	-
Myristic acid (MA)	-4.5	Ile269, Arg271, Leu362, NAD	Ser54, Asn56	-
Caprylic acid (CYA)	-4.2	Thyroxine 180, Lysine 330, Leucine 331, Phenylalanine 322	Lys323	-

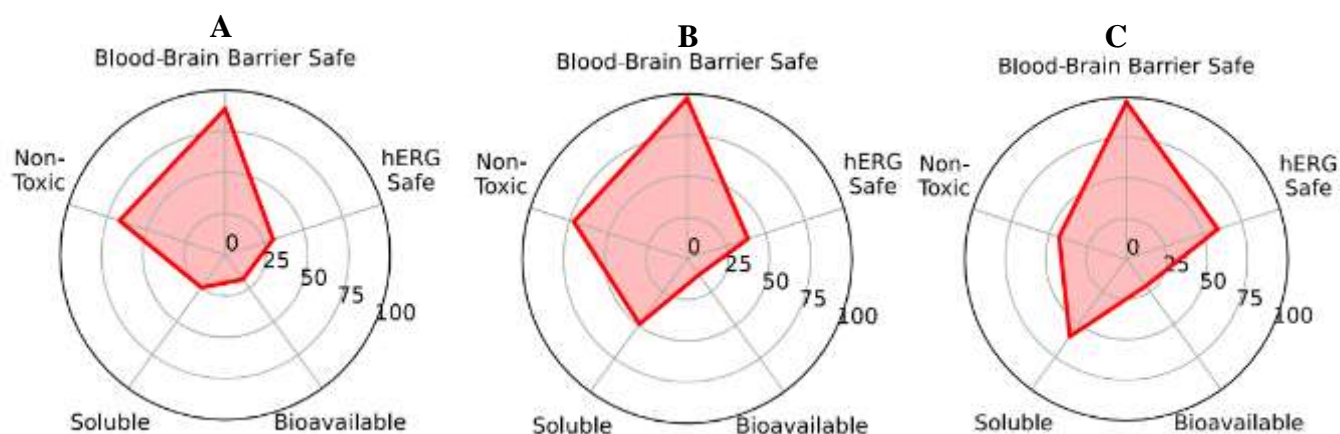


Figure 3: ADMET radial plot for TDF (A), QE (B), and TX (C).

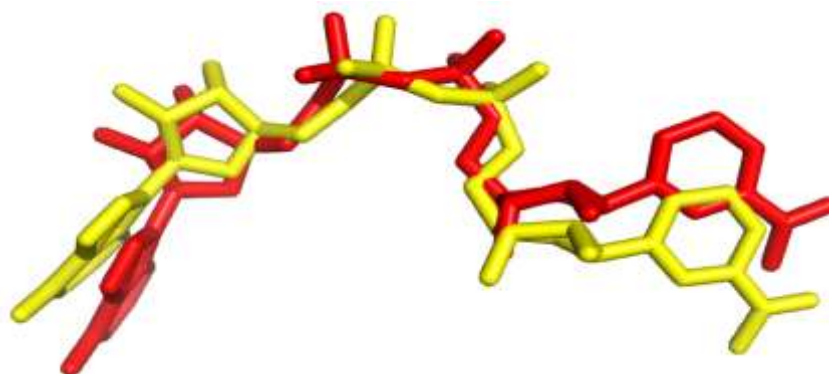


Figure 4: Conformation of NAD as a native ligand before (red) and after (yellow) the re-docking process.

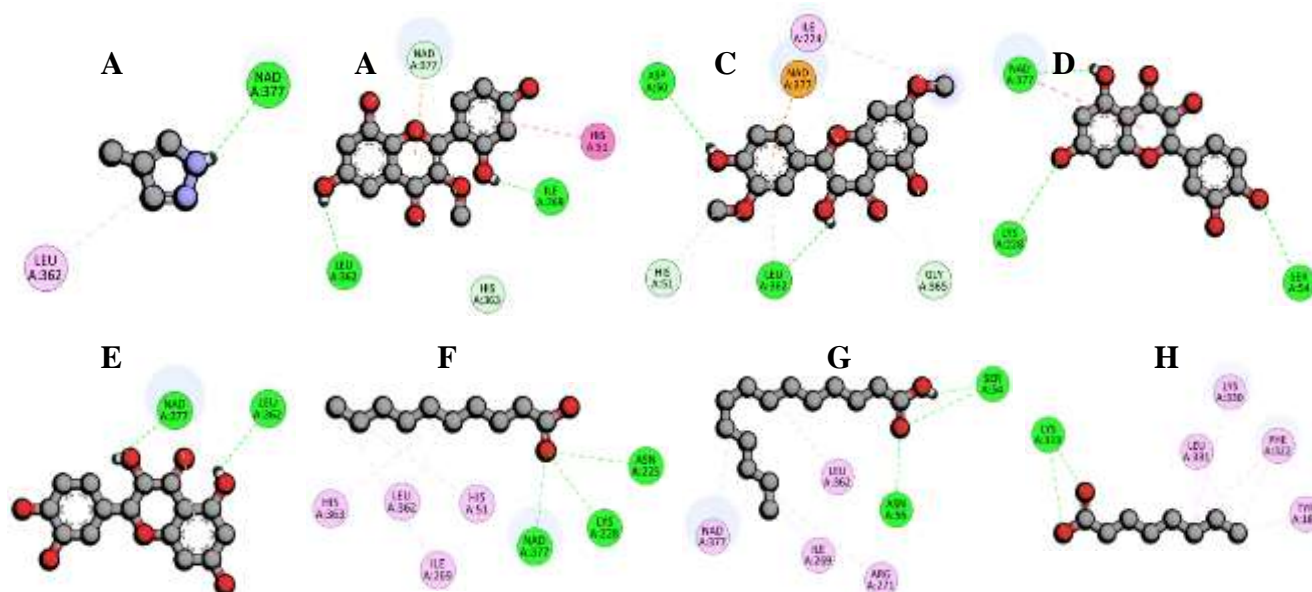


Figure 5: Interaction of the ligands Fomepizole (A), TMF (B), TDF (C), QE (D), TX (E), CRA (F), MA (G), and CYA (H) with the amino acid residues of the *alcohol dehydrogenase* enzyme.

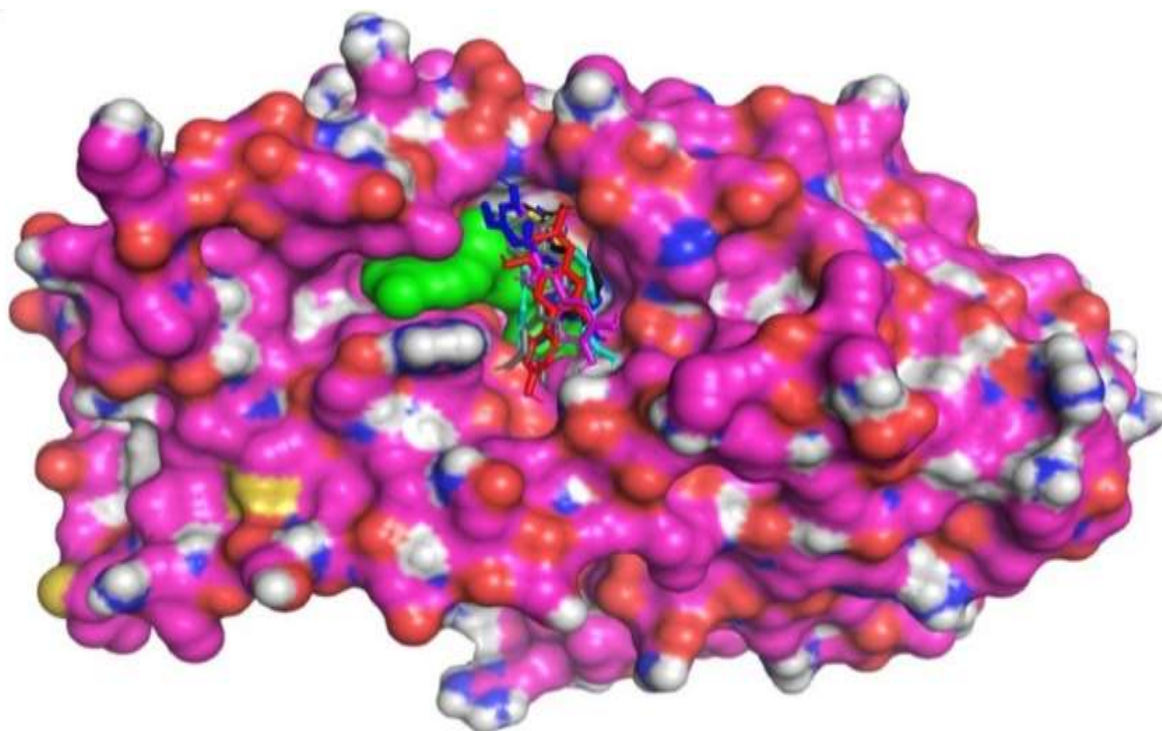


Figure 6: Inhibition sites of Fomepizole (yellow), TMF (red), TDF (blue), QE (purple), TX (gray), CRA (black), and MA (cyan) in the active site of *alcohol dehydrogenase* near NAD (green surface).

Molecular Dynamics (MD)

RMSD is the average displacement of atoms over a specific time interval. This represents the average distance between atoms (ligand) and protein. Based on Figure 7A, the most stable ligand for inhibiting ADH active site is QE, which remains stable below 3 Å up to 20 ns. RMSD values below 5 Å represent relative stability in molecular dynamics simulations. The value exceeding 5 Å imply significant conformational changes and major structural modifications, suggesting low stability.³⁶ QE is still considered a stable ligand up to 50 ns because RMSD value remains below 5 Å. However, TDF and TX are not good ADH inhibitors due to the irregular movement determined from RMSD values.

RMSF represents the local fluctuations of each residue in a protein, enabling the assessment of the stability of specific target protein residues during simulations.³⁷ Amino acid residues from 1 to 90 remain stable below 2.5 Å after the introduction of TDF, QE, and TX at the active site of ADH. Residues from 100 to 120 start to fluctuate above 2.5 Å (Figure 7B), suggesting flexible amino acids in the region. Ala317 and Phe319, which are used to stabilize NAD molecule (⁺) in the binding pocket, show mild fluctuations.³⁸ *Radius of Gyration* (Rg) serves as an indicator of density, stability, and structural folding.^{39,40} Figure 7C shows that ADH protein remains stable and compact with Rg value of approximately 20.5 Å when inhibited by the active compound for 50 ns. Concerning the number of hydrogen bonds, QE has an

average of 4 to 5 hydrogen bonds, which stabilize QE interactions in the active site of ADH protein. QE has the highest average number of hydrogen bonds compared to TDF and TX in Figure 7D. Hydrogen

bonds play a role in maintaining molecular stability, implying that the higher the number of hydrogen bonds, the more stable the molecule.^{41,42}

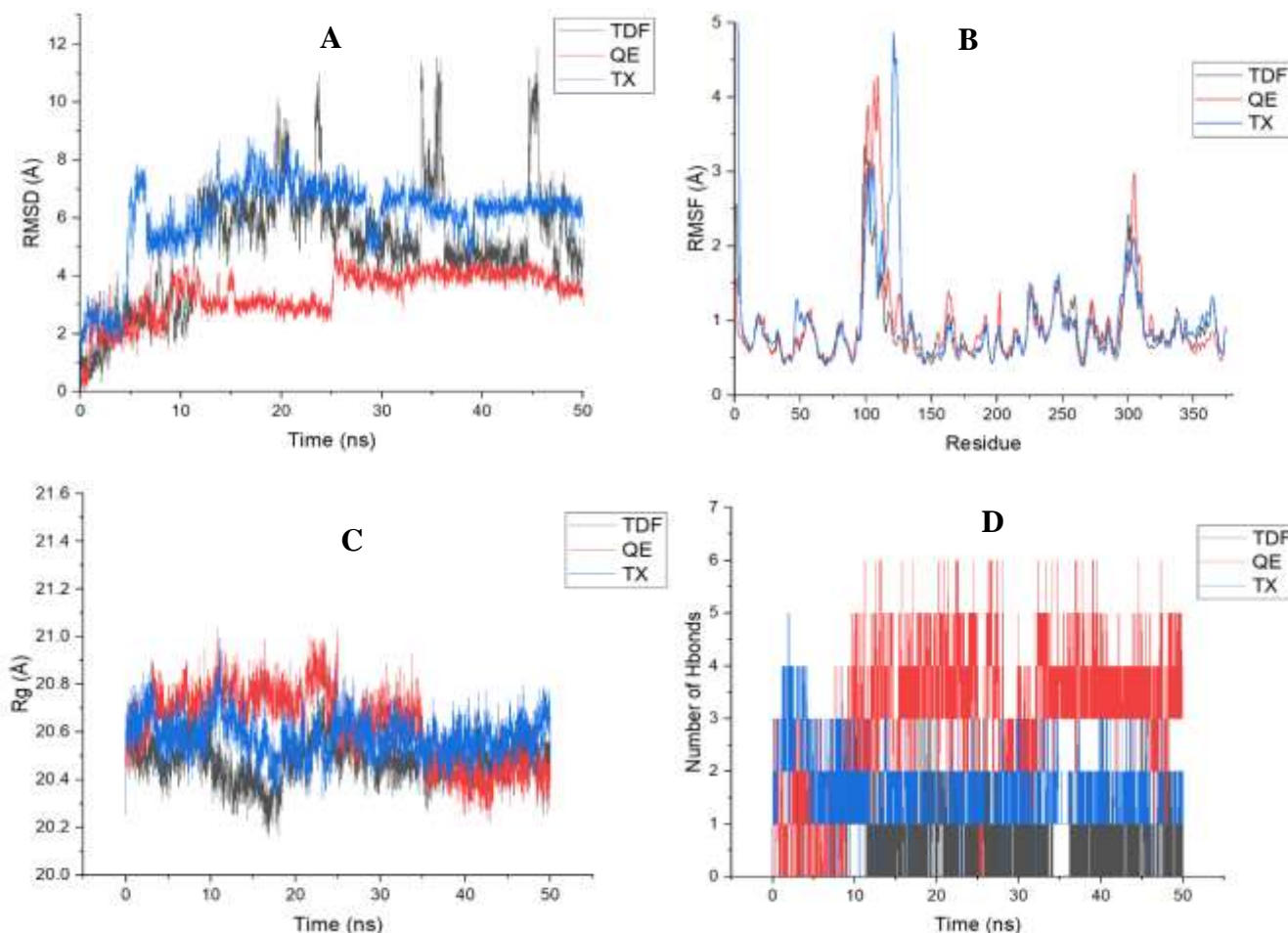


Figure 7: Molecular dynamics results of RMSD (A), RMSF (B), gyrate (C), and hydrogen bond count (D).

Conclusion

In conclusion, QE was identified as the most potent inhibitor of ADH enzyme isolated from *Pandanus conoideus* Lamk. Although other flavonoids such as TDF and TX showed significant binding affinity, QE presented better stability in molecular dynamics simulations. Stability, signified by low RMSD values during simulations, was a representation of better complex formation with ADH enzyme. Additionally, ADMET profile was favorable, suggesting the compound as non-toxic and safe regarding BBB permeability and hERG inhibition. The mechanism of action of QE was considered identical to the mechanism of the existing ADH inhibitor Fomepizole, due to the interaction with NAD molecules at the active site.

This study showed the potential of QE from *Pandanus conoideus* as a lead compound for the development of safer and more affordable ADH inhibitors derived from natural sources. Future investigations should focus on both *in vitro* and *in vivo* validations to confirm the inhibitory activity and pharmacological safety, as well as formulation strategies to improve the bioavailability. The efforts might contribute to the advancement of novel therapeutic methods for alcohol-related liver diseases and broaden the pharmacological relevance of endemic plants from Papua in global drug discovery.

Conflict of Interest

The authors declare no conflict of interest.

Authors' Declaration

The authors hereby declare that the work presented in this article is original and that any liability for claims relating to the content of this article will be borne by them.

Acknowledgements

The authors are grateful to the Faculty of Medicine, University of Papua, and the Government of Southwest Papua Province for their financial support (No: 2257/UN42/KS/2023) and provision of study facilities.

References

1. Rehm J, Shield KD. Global burden of alcohol use disorders and alcohol liver disease. *Biomedicines*. 2019; 7(4):7-6.
2. Bagnardi V, Blangiardo M, La Vecchia C, Corrao G. Alcohol consumption and the risk of cancer. *Alcohol Res Health*. 2001; 25(4):263 - 270.
3. Contreras-Zentella ML, Villalobos-García D, Hernández-Muñoz R. Ethanol metabolism in the liver, the induction of oxidant stress, and the antioxidant defense system. *Antioxidants*. 2022; 11(7):1-19.
4. Langhi C, Pedraz-Cuesta E, Haro D, Marrero PF, Rodríguez JC. Regulation of human class I alcohol dehydrogenases by bile acids. *J. Lipid Res*. 2013; 54(9):2475-2484.

5. Orywal K, Szmikowski M. Alcohol dehydrogenase and aldehyde dehydrogenase in malignant neoplasms. *Clin Exp Med*. 2017; 17(2):131–139.
6. Ying X, Ma K. Characterization of a zinc-containing alcohol dehydrogenase with stereoselectivity from the hyperthermophilic archaeon *Thermococcus guaymasensis*. *J Bacteriol*. 2011; 193(12):3009–3019.
7. Hadi S, Setiawan D, Viogenta P, Sunardi S, Nastiti K, Nisa K, Andiarsa D. Molecular docking and dynamics study of compounds from *Combretum indicum* var. B seeds as alcohol dehydrogenase inhibitors. *Trop J Nat Prod Res*. 2023; 7(11):5087–5096.
8. Pereira AR, de Souza JCP, Gonçalves AD, Pagnoncelli KC, Crespilho FN. Bioelectrooxidation of ethanol using NAD-dependent alcohol dehydrogenase on oxidized flexible carbon fiber arrays. *J. Braz Chem Soc*. 2017; 00(00):1–10.
9. Martinez-Hurtado JL, Calo-Fernandez B, Vazquez-Padin J. Preventing and mitigating alcohol toxicity: a review on protective substances. *Beverages (Basel)*. 2018; 4(39): 1 - 28.
10. Ashurst JV, Schaffer DH, Nappe TM. Methanol toxicity. In: StatPearls [internet]. Treasure Island (FL): StatPearls Publishing; 2025 [cited 2025 Aug 14]. Available from: <http://www.ncbi.nlm.nih.gov/books/NBK482121/>
11. Mégarbane B. Treatment of patients with ethylene glycol or methanol poisoning: focus on fomepizole. *Open Access Emerg Med*. 2010; 2:67–75.
12. Battistella M. Fomepizole as an antidote for ethylene glycol poisoning. *Ann Pharmacother*. 2002; 36:1085–1089.
13. Nasim N, Sandeep IS, Mohanty S. Plant-derived natural products for drug discovery: current approaches and prospects. *Nucleus (Calcutta)*. 2022; 65(3):399–411.
14. Lestari IT, Anggadiredja K, Garmana AN. Red fruit (*Pandanus conoideus* Lam) oil ameliorates streptozotocin-induced diabetic peripheral neuropathy by targeting the oxidative and inflammatory pathways in the spinal cord in a rat model. *Pharmacia*. 2024; 71:1–13.
15. Herdiyati Y, Atmaja HE, Satari MH, Kurnia D. Potential antibacterial flavonoid from red fruit (*Pandanus conoideus* Lam.) against pathogenic oral bacteria of *Enterococcus faecalis* ATCC 29212. *Open Dent J*. 2020; 14:433–439.
16. Astirin OP, Harini M, Handajani NS. The effect of crude extract of *Pandanus conoideus* Lam. var. yellow fruit on apoptosis expression of the breast cancer cells (T47D). *Biodiversitas*. 2009; 10(1):44–48.
17. Ainunnisa M, Fawwaz M, Pratama M. The antioxidant activity of red fruit juice (*Pandanus conoideus* Lam.) using the FRAP method. *Pharm Rep*. 2025; 4(1):5–10.
18. Damayanti L, Evaangelina IA, Laviana A, Herdiyati Y, Kurnia D. Antibacterial activity of buah merah (*Pandanus conoideus* Lam.) against bacterial oral pathogen of *Streptococcus sanguinis* ATCC10556, *Streptococcus mutans* ATCC 25175, and *Enterococcus faecalis* ATCC 29212: an in vitro study. *Open Dent J*. 2020; 14:113–119.
19. Umar AK. Flavonoid compounds of red fruit (*Pandanus conoideus* Lamk) as a potent SARS-CoV-2 main protease inhibitor: in silico approach. *Future J Pharm Sci*. 2021; 7(1):1–8.
20. Sirait MS, Warsiki E, Setyaningsih D. Potential of red fruit oil (*Pandanus conoideus* Lam.) as an antioxidant active packaging: a review. *IOP Conf. Ser.: Earth Environ. Sci*. 2021; 749:1–8.
21. Heriyanto, Gunawan IA, Fujii R, Maoka T, Shioi Y, Kameubun KMB, Limantara L, Brotosudarmo THP. Carotenoid composition in red fruit (*Pandanus conoideus* Lam.), an indigenous red fruit of the Papua islands. *J Food Compos Anal*. 2021; 96:3–31.
22. Lestari N, Junaidi L, Wijaya H, Wardayanie A, Ariningsih S. Development of processing technology for red fruit oil powder (*Pandanus conoideus* Lamk) as a food additive. *Warta IHP*. 2021; 38 (2):117–125.
23. Swanson K, Walther P, Leitz J, Mukherjee S, Wu JC, Shivanaraine RV, Zou J. ADMET-AI: a machine learning ADMET platform for evaluation of large-scale chemical libraries. *Bioinformatics*. 2024; 40(7):1–4.
24. Forli S, Huey R, Pique ME, Sanner MF, Goodsell DS, Olson AJ. Computational protein-ligand docking and virtual drug screening with the AutoDock suite. *Nat Protoc*. 2016; 11(5):905–919.
25. Hurley TD, Bosron WF, Stone CL, Amzel LM. Structures of three human beta alcohol dehydrogenase variants - correlations with their functional differences. *J Mol Biol*. 1994; 239(3):415–429.
26. Shamsian S, Sokouti B, Dastmalchi S. Benchmarking different docking protocols for predicting the binding poses of ligands complexed with cyclooxygenase enzymes and screening chemical libraries. *Bioimpacts*. 2024; 14(2):1–9.
27. Rao P, Shukla A, Parmar P, Rawal RM, Patel B, Saraf M, Goswami D. Reckoning a fungal metabolite, Pyranonigrin A as a potential Main protease (Mpro) inhibitor of novel SARS-CoV-2 virus identified using docking and molecular dynamics simulation. *Biophys Chem*. 2020; 264:1–10.
28. Karami TK, Hailu S, Feng S, Graham R, Gukasyan HJ. Eyes on Lipinski's rule of five: a new "rule of thumb" for physicochemical design space of ophthalmic drugs. *J Ocul Pharmacol Ther*. 2022; 38(1):43–55.
29. Wu K, Kwon SH, Zhou X, Fuller C, Wang X, Vadgama J, Wu Y. Overcoming challenges in small-molecule drug bioavailability: a review of key factors and approaches. *Int J Mol Sci*. 2024; 25(23):1–29.
30. Guengerich FP. Cytochrome P450 and chemical toxicology. *Chem Res Toxicol*. 2008; 21(1):70–83.
31. Mukherjee S, Swanson K, Walther P, Shivanaraine RV, Leitz J, Pang PD, Zou J, Wu JC. ADMET-AI enables interpretable predictions of drug-induced cardiotoxicity. *Circulation*. 2025; 151(3):285–287.
32. Nogawa H, Kawai T. HERG trafficking inhibition in drug-induced lethal cardiac arrhythmia. *Eur J Pharmacol*. 2014; 741:336–339.
33. Didigwu OK, Nnadi CO. Theoretical drug-likeness, pharmacokinetic and toxicities of phytotoxic terpenoids from the toxic plants-phytotoxins. *Trop J Nat Prod Res*. 2024; 8(10):8867–8873.
34. Vaidyanathan R, Sreedevi SM, Ravichandran K, Vinod SM, Krishnan YH, Babu LK, Parthiban PS, Baskar L, Perumal T, Rajaraman V, Arumugam G, Rajendran K, Mahalingam V. Molecular docking approach on the binding stability of derivatives of phenolic acids (DPAs) with human serum albumin (HSA): Hydrogen-bonding versus hydrophobic interactions or combined influences?. *JCIS Open*. 2023; 12:1–16.
35. Spassov DS. Binding affinity determination in drug design: insights from lock and key, induced fit, conformational selection, and inhibitor trapping models. *Int J Mol Sci*. 2024; 25(13):1–20.
36. Amrulloh LSWF, Harmastuti N, Prasetyo A, Herowati R. Analysis of molecular docking and dynamics simulation of mahogany (*Swietenia macrophylla* King) compounds against the PLpro Enzyme SARS-COV-2. *J. farm. ilmu kefarmasian Indones*. 2023; 10(3):347–359.
37. Fatriansyah JF, Rizqillah RK, Yandi MY, Fadilah, Sahlan M. Molecular docking and dynamics studies on propolis sulabiroid - A as a potential inhibitor of SARS-CoV-2. *J. King Saud Univ Sci*. 2022; 34(1):1–8.
38. Hayward S, Kitao A. Molecular dynamics simulations of NAD⁺-induced domain closure in horse liver alcohol dehydrogenase. *Biophys J*. 2006; 91(5):1823–1831.
39. Majumder R, Mandal M. Screening of plant-based natural compounds as a potential COVID-19 main protease inhibitor: an in silico docking and molecular dynamics simulation approach. *J Biomol Struct Dyn*. 2022; 40(2):696–711.

40. Rudnev VR, Nikolsky KS, Petrovsky DV, Kulikova LI, Kargatov AM, Malsagova KA, Stepanov AA, Kopylov AT, Kaysheva AL, Efimov AV. 3 β -corner stability by comparative molecular dynamics simulations. *Int J Mol Sci.* 2022; 23(19):1-13.
41. Pace CN, Scholtz JM, Grimsley GR. Forces stabilizing proteins. *FEBS Lett.* 2014; 588(14):2177–2184.
42. Hanoush DA, Al-Auqaili AH, Mansour M, Ghosh A. Molecular docking, molecular dynamic simulation and ADME of some plant extracts and their effects on COVID-19 Patients. *Trop J Nat Prod Res.* 2022; 6(8):1233-1240.